



Thermodiffusion: From kinetics to stochastic

F. Debbasch^{a,*}, J.P. Rivet^b

^a Université Paris 6, ERGA-LERMA, UMR 8112, 3, rue Galilée, F-94200 Ivry, France

^b UMR6202, Université de Nice Sophia-Antipolis, CNRS, Observatoire de la Côte d'Azur, B.P.4229, F-06304 Nice Cedex 04, France

ARTICLE INFO

Article history:

Received 5 November 2009

Received in revised form 24 January 2010

Available online 4 February 2010

Keywords:

Thermodiffusion

Kinetic theory

Fokker–Planck equation

ABSTRACT

The Boltzmann transport equation is used to obtain new effective stochastic descriptions of dilute gas diffusion in presence of temperature gradients. It is found that temperature gradients not only introduce a thermophoresis force, but also substantially modify the friction and noise acting on the diffusing particle. The various corrections are computed exactly and compared with each other and with the thermophoresis force.

© 2010 Elsevier B.V. All rights reserved.

1. Introduction

Thermodiffusion is diffusion generated by temperature gradients and is presently the object of active research, with applications ranging from chemistry to biology and petroleum extraction [1–5].

The first, purely macroscopic description of thermodiffusion [6] dates back to the nineteenth century, and assumes that diffusion currents are generally made up of two contributions, one proportional to density gradients (Fick law) and the other proportional to temperature gradients (Ludwig–Soret effect). This description can now be derived from a kinetic one based on Boltzmann equation.

Stochastic processes theory originated in the study of Brownian motion [7] and is known to be particularly efficient at modelling physical diffusions in general [8]. Various authors have thus considered stochastic models of thermodiffusion [9–11]. All models are based on generalizations of the standard Langevin equation. The models first proposed add the thermophoresis force to the standard Langevin [12] frictional and stochastic forces; in particular, these models presuppose that friction and noise coefficients are not modified by the presence of a temperature gradient. In many cases, however, these simple models fail to reproduce the observed values and even orders of magnitude of the Ludwig–Soret coefficient [11]. New stochastic models have thus been introduced in Refs. [13,14]. These models are more general than the previous ones [11] because they allow both friction and noise coefficients to depend on temperature gradients. But this dependence has not yet been confirmed or made explicit by theoretical, microscopic computations. In particular, it is not known how the mean temperature, the masses and the characteristic sizes of both solvent and solute particles enter this dependence.

The purpose of this article is to use kinetic theory to confirm that friction and noise coefficients generally depend on temperature gradients and to characterize this dependence in the high dilution limit, where first order contributions in the temperature gradient can be computed exactly. Our main results are that temperature gradients indeed modify the values of both friction and noise coefficients and that this new effect must *a priori* be taken into account if one wants to obtain theoretical predictions of Soret coefficients which better fit measured values.

* Corresponding author. Tel.: +33 144277286; fax: +33 144277287.

E-mail address: fabrice.debbasch@gmail.com (F. Debbasch).

2. General framework

2.1. Kinetics

Consider first a solvent gas S made of particles of mass m_S (conveniently called S -particles). For sufficiently high dilutions, all statistical properties of S are encoded in the one-particle distribution function f . If one neglects the internal structure of S -particles, f is a time-dependent function of six real degrees of freedom (for example, 3 position coordinates and 3 velocity components) and this function obeys the Boltzmann equation:

$$\frac{\partial f}{\partial t} + \mathbf{v} \cdot \nabla_{\mathbf{r}} f = \int d^3 v_1 \int |\mathbf{v} - \mathbf{v}_1| (f(\mathbf{v}')f(\mathbf{v}'_1) - f(\mathbf{v})f(\mathbf{v}_1)) d\sigma_S \quad (1)$$

where usual notations have been used [15,16]; in particular, \mathbf{v}' and \mathbf{v}'_1 are the velocities of the particles which result from the collision of two particles with initial velocities \mathbf{v} and \mathbf{v}_1 , and $d\sigma_S$ is the differential cross-section characterizing the collisions between two S -particles.

The mean free path λ_S of the S -particles is defined in terms of the total cross-section σ_S by $\lambda_S = \frac{1}{\sqrt{2}n_S\sigma_S}$, where n_S is the density of S -particles (*i.e.* the number of S -particles per unit volume). Approximating the interaction of S -particles by elastic collisions between hard spheres of radius R_S , one obtains:

$$\lambda_S = \frac{1}{\sqrt{2}n_S\pi(2R_S)^2}. \quad (2)$$

Suppose that the gas S is at rest in a reference frame \mathcal{R} but that a non uniform temperature field $T(\mathbf{r})$ is maintained in S ; the distribution f_T describing this situation is a time-independent solution of (1) which reduces to the standard Maxwell distribution for vanishing temperature gradients. This distribution can be expanded in terms of the dimensionless quantity $\lambda_S \nabla T / T$ and reads, at first order:

$$f_T(\mathbf{v}_S) = \left(\frac{2\pi k_B T}{m_S} \right)^{-\frac{3}{2}} \exp\left(-\frac{m_S v_S^2}{2k_B T}\right) \left\{ 1 - \frac{16}{5\sqrt{2\pi}} \left(\frac{m_S v_S^2}{2k_B T} - \frac{5}{2} \right) \sqrt{\frac{m_S}{k_B T}} \mathbf{v}_S \cdot \frac{\lambda_S \nabla T}{T} \right\}, \quad (3)$$

where $k_B T$ is the Boltzmann factor. Note that the kinematic shear viscosity $\nu_S(T)$ is proportional to λ_S and to the thermal velocity of the S -particle [15]: $\nu_S(T) = \frac{5\sqrt{2\pi}}{16} \lambda_S \sqrt{\frac{k_B T}{m_S}}$, and that (3) is thus sometimes expressed in terms of $\nu_S(T)$ [11].

We will suppose that (3) correctly describes the state of the solvent S ; this amounts to supposing that the temperature field T varies on scales much larger than the mean free path λ_S *i.e.* on macroscopic scales only.

Consider now particles of mass m_B , conveniently called Brownian or B -particles, diffusing in the above solvent through short-range interactions. We suppose that there are sufficiently few Brownian particles in S to neglect interactions between B -particles and between more than one B - and one S -particle at a time. All properties of diffusion can then be recovered by studying the motion of a single, arbitrary B -particle and the statistical properties of this motion are entirely characterized by expression (3) for the solvent distribution f_T and by a law characterizing the short-range interaction between a B - and an S -particle. We neglect the internal structure of B -particles and assume, in coherence with (2), that the short-range interaction between a B - and an S -particle can be modelled as an elastic collision between hard spheres and that the associated sphere radius for B -particles is R_B .

2.2. Stochastics

In the above model, the trajectory of a B -particle is a succession of line segments started and ended by collisions with S -particles. At a fixed initial momentum \mathbf{p}_B of the B -particle before such a collision, the momentum loss $\mathbf{q}_B = \mathbf{p}_B - \mathbf{p}'_B$ of the B -particle during the collision is a random variable whose distribution depends on the collision cross-section and on the distribution of S -particles. Langevin-like equations (Ito processes [17]) are driven by Gaussian noises. Approximating the motion of a B -particle by a Langevin-like equation thus comes down to approximating, for each \mathbf{p}_B , the distribution of the momentum loss \mathbf{q}_B by a Gaussian. The law of a stochastic process defined by such a Langevin equation is described by a distribution function ϕ of the time t and of the position \mathbf{r}_B and momentum \mathbf{p}_B of a B -particle; this function obeys the Fokker–Planck equation [17]:

$$\frac{\partial \phi}{\partial t} + \frac{p_B^i}{m} \frac{\partial \phi}{\partial r_B^i} = \frac{\partial}{\partial p_B^i} \left(-F^i \phi + \frac{\partial}{\partial p_B^j} (D^{ij} \phi) \right) \quad (4)$$

where \mathbf{F} is the deterministic part of the force experienced by the B -particle, and D is the noise tensor. This force \mathbf{F} and the noise tensor D can be computed from the expectation (mean value) of \mathbf{q}_B and $\mathbf{q}_B \otimes \mathbf{q}_B$, respectively.

The exact computation of the expectations $\langle \mathbf{q}_B \rangle$ and $\langle \mathbf{q}_B \otimes \mathbf{q}_B \rangle$, and thus, of \mathbf{F} and D is presented in Appendix A. The next section offers a qualitative and graphical presentation of the results. The force \mathbf{F} splits into the so-called thermophoresis force and a friction force. The presented results confirm that friction and noise coefficients generically depend on the temperature gradient.

3. Results

As detailed in [Appendix A](#), the hard sphere Boltzmann model delivers explicit expressions at first order in ∇T for the deterministic part \mathbf{F} of the force experienced by a B -particle with velocity \mathbf{v}_B , and for the noise tensor D . These expressions are of the form:

$$\mathbf{F} = \kappa(T, \mathbf{v}_B^2) \nabla T - (\alpha_0(T, \mathbf{v}_B^2) + \alpha_1(T, \mathbf{v}_B^2) \mathbf{v}_B \cdot \nabla T) \mathbf{v}_B, \quad (5)$$

and

$$D = (\sigma_0(T, \mathbf{v}_B^2) + \sigma_1(T, \mathbf{v}_B^2) \mathbf{v}_B \cdot \nabla T) \mathcal{E} + (\sigma_2(T, \mathbf{v}_B^2) + \sigma_3(T, \mathbf{v}_B^2) \mathbf{v}_B \cdot \nabla T) \mathbf{v}_B \otimes \mathbf{v}_B + \sigma_4(T, \mathbf{v}_B^2) \frac{\mathbf{v}_B \otimes \nabla T + \nabla T \otimes \mathbf{v}_B}{2} \quad (6)$$

where \mathcal{E} is the (inverse) euclidean metric tensor ($\mathcal{E}^{ij} = 1$ if $i = j$ and 0 otherwise). The tensor D depends on ∇T if at least one of the coefficients σ_1 , σ_3 or σ_4 does not vanish. Naturally, all coefficients introduced above also depend on the masses m_B and m_S , and on the characteristic radii R_B and R_S . The expressions of the coefficients in (5) and (6) are more readable if the following conventions are done:

- \mathbf{u}_B denotes the dimensionless velocity of the B -particles: $\mathbf{u}_B = \mathbf{v}_B \sqrt{m_S/k_B T}$. Note that the velocity scale $k_B T/m_S$ chosen to make \mathbf{u}_B dimensionless is the thermal velocity of S -particles. Thus, when the B -particles have a much larger mass than the S -particles, $|\mathbf{u}_B|$ is much smaller than unity.
- u_B and v_B denote the moduli of \mathbf{u}_B and \mathbf{v}_B .
- μ denotes $(m_S^{-1} + m_B^{-1})^{-1}$.
- $\xi(x)$ stands for $e^{-x^2/2}$, and $\zeta(x)$ for $\sqrt{\frac{\pi}{2}} \frac{\text{erf}(x/\sqrt{2})}{x}$, where analytical continuation is implied for $x = 0$.

With this notation, the exact expressions for the coefficients in (5) and (6), and their expansions for small u_B are:

- Thermophoresis coefficient:

$$\begin{aligned} \kappa(T, v_B^2) &\equiv \tilde{\kappa}(T, u_B^2) = 3n_S \frac{v_S(T)}{T} \sqrt{\frac{2\pi k_B T}{m_S}} \mu (R_B + R_S)^2 \left(\frac{1 - u_B^2}{u_B^2} \zeta(u_B) - \frac{1}{u_B^2} \xi(u_B) \right) \\ &= n_S \frac{v_S(T)}{T} \sqrt{\frac{2\pi k_B T}{m_S}} \mu (R_B + R_S)^2 \left(-2 + \frac{1}{5} u_B^2 \right) + \mathcal{O}(u_B^4). \end{aligned} \quad (7)$$

- Friction coefficient:

$$\begin{aligned} \alpha_0(T, v_B^2) &\equiv \tilde{\alpha}_0(T, u_B^2) = n_S \sqrt{\frac{2\pi k_B T}{m_S}} \mu (R_B + R_S)^2 \left(\frac{-1 + 2u_B^2 + u_B^4}{u_B^2} \zeta(u_B) + \frac{1 + u_B^2}{u_B^2} \xi(u_B) \right) \\ &= \frac{4}{3} n_S \sqrt{\frac{2\pi k_B T}{m_S}} \mu (R_B + R_S)^2 \left(2 + \frac{1}{5} u_B^2 \right) + \mathcal{O}(u_B^4). \end{aligned} \quad (8)$$

- Thermally induced correction to the friction term:

$$\begin{aligned} \alpha_1(T, v_B^2) &\equiv \tilde{\alpha}_1(T, u_B^2) = 6\pi n_S \frac{v_S(T)}{T} \sqrt{\frac{m_S}{2\pi k_B T}} \mu (R_B + R_S)^2 \left(\frac{3 - u_B^2}{u_B^4} \zeta(u_B) - \frac{3}{u_B^4} \xi(u_B) \right) \\ &= \frac{6\pi}{5} n_S \frac{v_S(T)}{T} \sqrt{\frac{m_S}{2\pi k_B T}} \mu (R_B + R_S)^2 \left(-\frac{2}{3} + \frac{1}{7} u_B^2 \right) + \mathcal{O}(u_B^4). \end{aligned} \quad (9)$$

- Noise coefficient:

$$\begin{aligned} \sigma_0(T, v_B^2) &\equiv \tilde{\sigma}_0(T, u_B^2) = \frac{1}{12\pi} n_S \left(\frac{2\pi k_B T}{m_S} \right)^{\frac{3}{2}} \mu^2 (R_B + R_S)^2 \\ &\quad \times \left(\frac{-3 + 9u_B^2 + 9u_B^4 + u_B^6}{u_B^2} \zeta(u_B) + \frac{3 + 8u_B^2 + u_B^4}{u_B^2} \xi(u_B) \right) \\ &= \frac{1}{12\pi} n_S \left(\frac{2\pi k_B T}{m_S} \right)^{\frac{3}{2}} \mu^2 (R_B + R_S)^2 \left(16 + \frac{24}{5} u_B^2 \right) + \mathcal{O}(u_B^4). \end{aligned} \quad (10)$$

- Thermally induced correction to the noise term:

$$\begin{aligned} \sigma_1(T, v_B^2) \equiv \tilde{\sigma}_1(T, u_B^2) &= \frac{9}{4} n_S \frac{v_S(T)}{T} \sqrt{\frac{2\pi k_B T}{m_S}} \mu^2 (R_B + R_S)^2 \left(\frac{3 - 2u_B^2 + u_B^4}{u_B^4} \zeta(u_B) + \frac{-3 + u_B^2}{u_B^4} \xi(u_B) \right) \\ &= \frac{3}{5} n_S \frac{v_S(T)}{T} \sqrt{\frac{2\pi k_B T}{m_S}} \mu^2 (R_B + R_S)^2 \left(2 - \frac{1}{7} u_B^2 \right) + \mathcal{O}(u_B^4). \end{aligned} \quad (11)$$

- Second order noise coefficient:

$$\begin{aligned} \sigma_2(T, v_B^2) \equiv \tilde{\sigma}_2(T, u_B^2) &= \frac{1}{2} n_S \sqrt{\frac{2\pi k_B T}{m_S}} \mu^2 (R_B + R_S)^2 \\ &\quad \times \left(\frac{3 - 3u_B^2 + 3u_B^4 + u_B^6}{u_B^4} \zeta(u_B) + \frac{-3 + 2u_B^2 + u_B^4}{u_B^4} \xi(u_B) \right) \\ &= \frac{4}{5} n_S \sqrt{\frac{2\pi k_B T}{m_S}} \mu^2 (R_B + R_S)^2 \left(2 + \frac{1}{7} u_B^2 \right) + \mathcal{O}(u_B^4). \end{aligned} \quad (12)$$

- Thermally induced correction to the second order noise term:

$$\begin{aligned} \sigma_3(T, v_B^2) \equiv \tilde{\sigma}_3(T, u_B^2) &= \frac{9\pi}{2} n_S \frac{v_S(T)}{T} \sqrt{\frac{m_S}{2\pi k_B T}} \mu^2 (R_B + R_S)^2 \left(\frac{15 - 6u_B^2 + u_B^4}{u_B^6} \zeta(u_B) + \frac{-15 + u_B^2}{u_B^6} \xi(u_B) \right) \\ &= \frac{2\pi}{35} n_S \frac{v_S(T)}{T} \sqrt{\frac{m_S}{2\pi k_B T}} \mu^2 (R_B + R_S)^2 (6 - u_B^2) + \mathcal{O}(u_B^4). \end{aligned} \quad (13)$$

- Thermally induced noise term:

$$\begin{aligned} \sigma_4(T, v_B^2) \equiv \tilde{\sigma}_4(T, u_B^2) &= \frac{3}{2} n_S \frac{v_S(T)}{T} \sqrt{\frac{2\pi k_B T}{m_S}} \mu^2 (R_B + R_S)^2 \left(\frac{9 + 9u_B^2 - 45u_B^4 - 36u_B^6 + 4u_B^8 + u_B^{10}}{u_B^4} \zeta(u_B) \right. \\ &\quad \left. + \frac{-9 - 12u_B^2 - 37u_B^4 + 3u_B^6 + u_B^8}{u_B^4} \xi(u_B) \right) \\ &= \frac{6}{5} n_S \frac{v_S(T)}{T} \sqrt{\frac{2\pi k_B T}{m_S}} \mu^2 (R_B + R_S)^2 \left(-98 - \frac{71}{7} u_B^2 \right) + \mathcal{O}(u_B^4). \end{aligned} \quad (14)$$

Some comments are now in order. The new stochastic process introduced in Refs. [13,14] to model thermodiffusion are general enough to incorporate thermally induced corrections to the friction coefficient and to the noise term. The analytic calculation presented here shows that such correction indeed exists for hard sphere Brownian particles interacting with a dilute gas of hard sphere particles, at least in presence of a macroscopic thermal gradient (*i.e.* a thermal gradient with variation scale much larger than the mean free path). It is obviously interesting to compare the orders of magnitudes of these new thermally induced corrections and of the usual thermophoresis force. For example, the thermally induced correction to the friction term $(\alpha_1 \mathbf{v}_B \cdot \nabla T) \mathbf{v}_B$ is linear in the thermal gradient and can be compared naturally with the thermophoresis force. Let us define the ratio $\rho_a(T, \mathbf{v}_B)$ of the two by:

$$\rho_a(T, \mathbf{v}_B) = \frac{|\alpha_1(T, \mathbf{v}_B^2) (\mathbf{v}_B \cdot \nabla T) \mathbf{v}_B|}{|\kappa(T, \mathbf{v}_B^2) \nabla T|}. \quad (15)$$

In the most favorable case (\mathbf{v}_B parallel to ∇T), this ratio can be expressed as a function $\tilde{\rho}_a(u_B^2)$ of the dimensionless variable $u_B^2 = \mathbf{v}_B^2 m_S / k_B T$ only. Eqs. (7) and (9) yield the following explicit expression for $\rho_a(u_B^2)$:

$$\rho_a(T, \mathbf{v}_B) \equiv \tilde{\rho}_a(u_B^2) = \frac{|(3 - u_B^2) \zeta(\sqrt{u_B^2}) - 3 \xi(\sqrt{u_B^2})|}{|(1 - u_B^2) \zeta(\sqrt{u_B^2}) - \xi(\sqrt{u_B^2})|}. \quad (16)$$

A priori, *B*-particles can have velocities with arbitrary moduli. However, if we assume that the *B*-particles are in statistical equilibrium with the surrounding gas, their most probable velocity scales like $\sqrt{k_B T / m_B}$, and the dimensionless variable u_B^2 which appears in Expressions (7)–(14) scales like the mass ratio m_S / m_B . This yields a way to estimate the ratio ρ_a as a function of the mass ratio only. Fig. 1 shows how this estimate of the ratio ρ_a varies as a function of the mass ratio m_S / m_B .

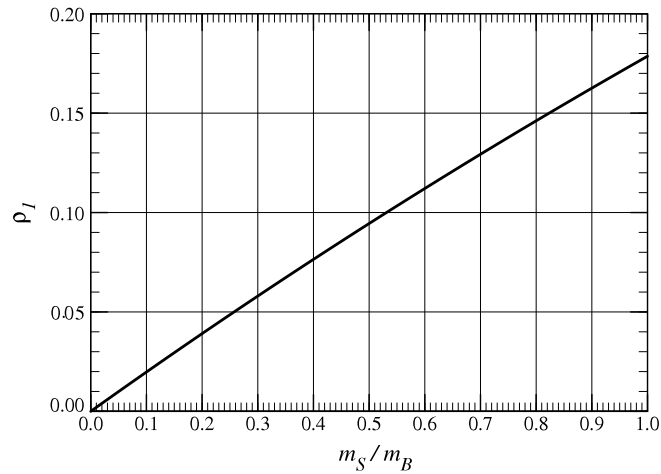


Fig. 1. Relative importance of the thermally induced correction to the friction term and of the thermophoresis term, as a function of the mass ratio.

This shows that the correction to the friction force induced by the temperature gradient cannot be neglected if the mass of *B*-particles is not very large when compared with the mass of the *S*-particles.

The comparison of the thermally induced noise terms to the thermophoresis force is not as straightforward as for the deterministic terms. A glance at Eq. (4) suggests that the deterministic force terms are to be compared with the derivative of the noise terms, with respect to the momentum \mathbf{p}_B of the Brownian particle. Consequently, to compare the new thermally induced corrections $\sigma_1(\mathbf{v}_B \cdot \nabla T)\boldsymbol{\varepsilon}$, $\sigma_3(\mathbf{v}_B \cdot \nabla T)\mathbf{v}_B \otimes \mathbf{v}_B$ and $\sigma_4(\mathbf{v}_B \otimes \nabla T + \nabla T \otimes \mathbf{v}_B)/2$ to the usual thermophoresis term $\kappa(T, \mathbf{v}_B^2)\nabla T$, we introduce the following dimensionless ratios:

$$\rho_b(T, \mathbf{v}_B) = \frac{\left| \frac{1}{m_B} \nabla_{\mathbf{v}_B} \cdot (\sigma_1(T, \mathbf{v}_B^2)(\mathbf{v}_B \cdot \nabla T)\boldsymbol{\varepsilon}) \right|}{\left| \kappa(T, \mathbf{v}_B^2)\nabla T \right|}, \tag{17}$$

$$\rho_c(T, \mathbf{v}_B) = \frac{\left| \frac{1}{m_B} \nabla_{\mathbf{v}_B} \cdot (\sigma_3(T, \mathbf{v}_B^2)(\mathbf{v}_B \cdot \nabla T)\mathbf{v}_B \otimes \mathbf{v}_B) \right|}{\left| \kappa(T, \mathbf{v}_B^2)\nabla T \right|}, \tag{18}$$

and

$$\rho_d(T, \mathbf{v}_B) = \frac{\left| \frac{1}{m_B} \nabla_{\mathbf{v}_B} \cdot (\sigma_4(T, \mathbf{v}_B^2)(\mathbf{v}_B \otimes \nabla T + \nabla T \otimes \mathbf{v}_B)/2) \right|}{\left| \kappa(T, \mathbf{v}_B^2)\nabla T \right|}. \tag{19}$$

In the most favorable case (\mathbf{v}_B parallel to ∇T), these ratios can be expressed as function $\tilde{\rho}_b(u_B^2, \eta)$, $\tilde{\rho}_c(u_B^2, \eta)$ and $\tilde{\rho}_d(u_B^2, \eta)$ of the dimensionless variable $u_B^2 = \mathbf{v}_B^2 m_S/k_B T$ and of the mass ratio η . Eqs. (7) and (11)–(14) yield the following explicit expression for these ratios:

$$\rho_b(T, \mathbf{v}_B, \eta) \equiv \tilde{\rho}_b(u_B^2, \eta) = \frac{3\eta}{1+\eta} \frac{\left| (-3 + u_B^2)\zeta(\sqrt{u_B^2}) + 3\xi(\sqrt{u_B^2}) \right|}{\left| u_B^2(1 - u_B^2)\zeta(\sqrt{u_B^2}) - u_B^2\xi(\sqrt{u_B^2}) \right|}, \tag{20}$$

$$\rho_c(T, \mathbf{v}_B, \eta) \equiv \tilde{\rho}_c(u_B^2, \eta) = \frac{3\eta}{1+\eta} \frac{\left| (-15 + 3u_B^2)\zeta(\sqrt{u_B^2}) + (15 + 2u_B^2)\xi(\sqrt{u_B^2}) \right|}{\left| u_B^2(1 - u_B^2)\zeta(\sqrt{u_B^2}) - u_B^2\xi(\sqrt{u_B^2}) \right|}, \tag{21}$$

and

$$\rho_d(T, \mathbf{v}_B, \eta) \equiv \tilde{\rho}_d(u_B^2, \eta) = \frac{\eta}{2(1+\eta)} \times \frac{\left| (-18 - 9u_B^2 - 36u_B^6 + 8u_B^8 + 3u_B^{10})\zeta(\sqrt{u_B^2}) + (18 + 15u_B^2 - 35u_B^4 + 5u_B^6 + 3u_B^8)\xi(\sqrt{u_B^2}) \right|}{\left| u_B^2(1 - u_B^2)\zeta(\sqrt{u_B^2}) - u_B^2\xi(\sqrt{u_B^2}) \right|}. \tag{22}$$

Using the same argument as for ρ_a , the most probable value of the squared dimensionless velocity u_B^2 of the Brownian particles scales like the mass ration η . The resulting estimate of the ratios ρ_b , ρ_c and ρ_d can be plotted as a functions of the

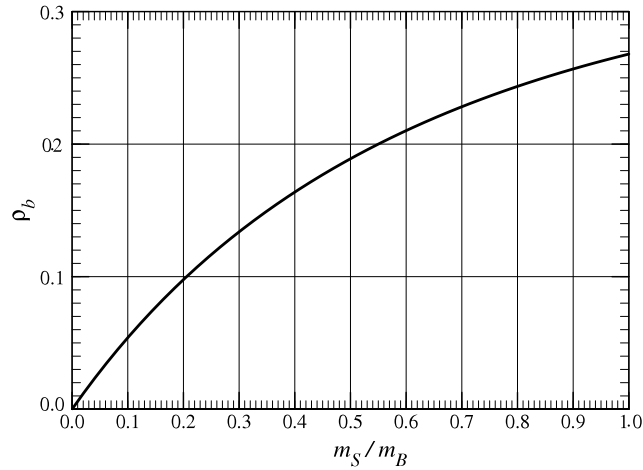


Fig. 2. Relative importance of the thermally induced correction to the diagonal noise term, and of the thermophoresis term, as a function of the mass ratio.

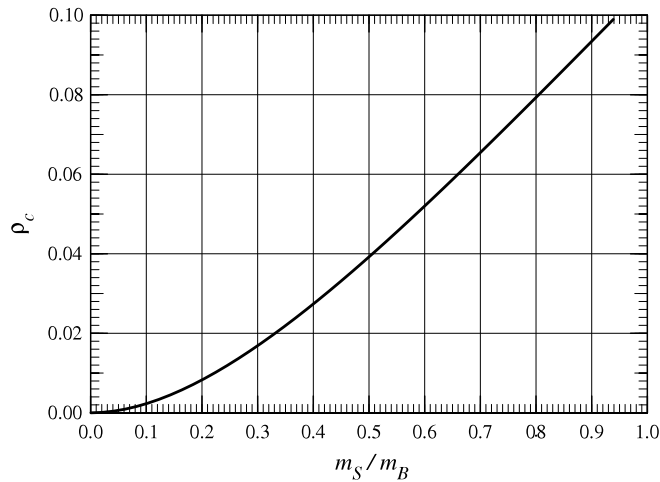


Fig. 3. Relative importance of the thermally induced correction to the $\mathbf{u}_B \otimes \mathbf{u}_B$ noise term, and of the thermophoresis term, as a function of the mass ratio.

mass ratio only (see Figs. 2–4). It is worth noting that ρ_b and ρ_c are relatively small when the mass ratio is not close to one. Thus, in the most common situation where the Brownian particles are much heavier than the solute particles, the thermally induced corrections to the diagonal noise term and to the $\mathbf{v}_B \otimes \mathbf{v}_B$ noise term can be neglected. However, this is not the case for the $\mathbf{v}_B \otimes \nabla T$ noise term, as revealed by the study of the ratio ρ_d . Indeed, this contribution of the thermal gradient to the noise term is as high as 30% of the thermophoresis force, even when the mass ratio is only 0.01 (Brownian particles 100 times heavier than solute particles).

4. Conclusion

We have used the Boltzmann equation to obtain new effective stochastic descriptions of dilute gas diffusions in presence of temperature gradients. Our main result is that temperature gradients substantially modify the friction and noise acting on the diffusing particle. We have computed the various corrections exactly at first order in the temperature gradients; we have also compared these corrections with each other and with the thermophoresis force. These new results strongly support the recent prediction [13,14] that conventional stochastic models [9,10] of diffusion under macroscopic temperature gradients are not general enough and that richer, more realistic stochastic models are needed.

This work can be prolonged in various directions. First and foremost, one should extend it outside the dilute gas regime to include, not only non dilute gases but also liquids; this will be probably best achieved through molecular dynamics simulations. One also wonders how the results presented in this article are modified if the temperature gradient driving the diffusion depends on time. For dilute gases, the first step in addressing this problem would be to find non stationary solutions of the Boltzmann equation describing the evolution of the solvent under the time-dependent temperature gradient. Finally, a relativistic extension of this work is also mandatory, if only to develop realistic stochastic models of diffusions in relativistic

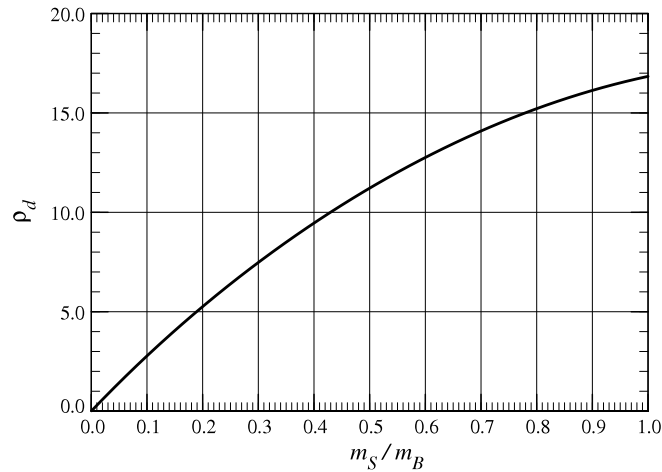


Fig. 4. Relative importance of the $\mathbf{u}_B \otimes \nabla T$ noise term, and the thermophoresis term, as a function of the mass ratio.

stars [18]; this extension should be based upon the purely kinetic description of relativistic thermodiffusion presented in Refs. [19–21].

Acknowledgement

Part of this work has been funded by the ANR grant “ProbaGeo”.

Appendix A. Computation of the expectations

A.1. Notations

In the following computation, we consider a Brownian particle (or B -particle) with mass m_B , which behaves under collisions as a hard sphere with radius R_B . It is immersed in a solvent gas of S -particles with mass m_S , which behave as hard spheres with radius R_S . The inertial frame in which the solvent gas is at rest is denoted by \mathcal{R} . We consider an elastic binary collision between the B -particle (Particle B) and an S -particle. Let \mathcal{R}^* be the proper reference frame of the two colliding particles, in which the total momentum of the two particles vanish. The momenta of B - and S -particles in \mathcal{R} are denoted by \mathbf{p}_B and \mathbf{p}_S before collision, and by \mathbf{p}'_B and \mathbf{p}'_S after collision. In the proper reference frame \mathcal{R}^* , these momenta are denoted by $\tilde{\mathbf{p}}_B$, $\tilde{\mathbf{p}}_S$, $\tilde{\mathbf{p}}'_B$ and $\tilde{\mathbf{p}}'_S$.

For the individual collision under consideration, we use $\tilde{\mathbf{p}}_B$ to define a unit vector $\hat{\mathbf{z}} = \tilde{\mathbf{p}}_B/\tilde{p}_B$ along which the space coordinate z can be measured. Two orthogonal unit vectors $\hat{\mathbf{x}}$ and $\hat{\mathbf{y}}$, perpendicular to $\hat{\mathbf{z}}$ are also defined to measure x and y space coordinates (see Fig. 5). The incidence plane ($x'z$) of the collision makes an angle ϕ with the arbitrary reference plane (xz), and the impact parameter is denoted b (see also Fig. 6).

Fig. 6 describes the geometry of the collision in the incidence plane ($x'z$). The y' direction is perpendicular to the plane of the figure, directed towards the reader. If the collision is assumed elastic (energy is conserved), the post-collision momenta $\tilde{\mathbf{p}}'_B$ and $\tilde{\mathbf{p}}'_S$ in \mathcal{R}^* can be deduced from the pre-collision momenta $\tilde{\mathbf{p}}_B$ and $\tilde{\mathbf{p}}_S$ by a rotation of angle $\alpha - \pi$. The angle α depends on the impact parameter b in the following manner. The impact parameter and the contact angle θ are linked by the simple geometric relation:

$$\sin \theta = \frac{b}{R_B + R_S}. \quad (23)$$

Under the hard sphere elastic collision hypothesis (specular reflection on the common tangent plane in the proper reference frame), the angles θ and α are linked by the relation:

$$\alpha = 2\theta. \quad (24)$$

A.2. Computation of the expectation $\langle \mathbf{q}_B \rangle$

Let us compute the ensemble-averaged momentum $\langle \mathbf{q}_B \rangle$ lost by the Brownian particle through collisions with solvent particles during a certain time interval δt . Let \mathbf{v}_B and \mathbf{v}_S be the initial velocities of colliding B - and S -particles in \mathcal{R} . The number of gas particles with velocity \mathbf{v}_S colliding the Brownian particle during δt is:

$$d^2N = n_S |\mathbf{v}_B - \mathbf{v}_S| \delta t b d\mathbf{b} d\phi, \quad (25)$$

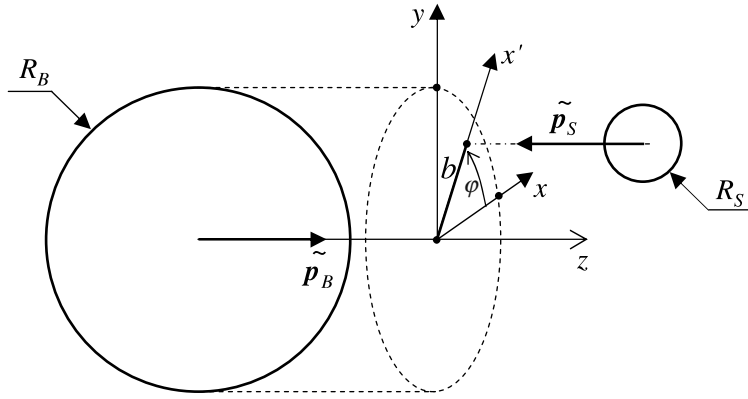


Fig. 5. 3D perspective view of a typical binary collision in the proper reference frame \mathcal{R}^* of the pair of particles. The Brownian particle (B -particle) has radius R_B , and the solvent gas particle (S -particle) has radius R_S . The z axis lies along the initial momentum $\tilde{\mathbf{p}}_B$ of the B -particle in \mathcal{R}^* . The x and y axes are two perpendicular arbitrary directions lying in the plane perpendicular to the z axis. b is the impact parameter, and ϕ is the angle of the incidence plane ($x'z$) with respect to the reference plane (xz).

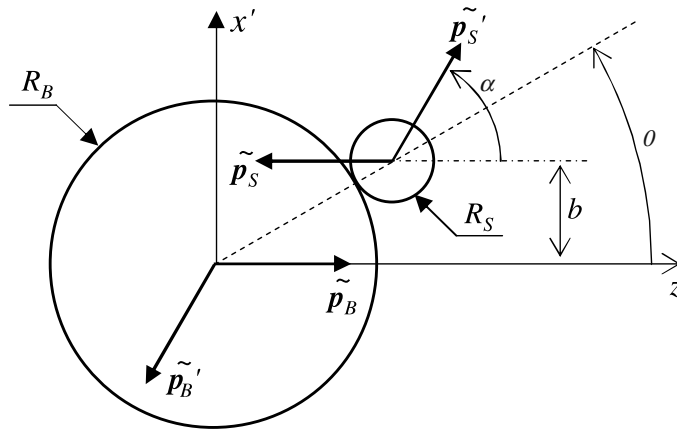


Fig. 6. 2D geometry of a typical collision in \mathcal{R}^* , viewed in the incidence plane ($x'z$). $\tilde{\mathbf{p}}_B$ and $\tilde{\mathbf{p}}_S$ are the momenta of B - and S -particles in \mathcal{R}^* before collision. $\tilde{\mathbf{p}}'_B$ and $\tilde{\mathbf{p}}'_S$ are the momenta in \mathcal{R}^* after collision.

where n_S is the number of particles S per unit volume. The impact parameter and the angle ϕ are defined in Figs. 5 and 6. From (23) and (24), the impact parameter can be expressed in terms of the angle α as : $\frac{b^2}{2} = \left(\frac{R_B+R_S}{2}\right)^2 (1 - \cos \alpha)$. Consequently, the surface element bdb in (25) can be expressed as: $bdb = \left(\frac{R_B+R_S}{2}\right)^2 \sin \alpha d\alpha$.

The momenta $\tilde{\mathbf{p}}_B$ and $\tilde{\mathbf{p}}'_B$ of the Brownian particle in \mathcal{R}^* , before and after the collision, and the momentum loss $\mathbf{q}_B = \mathbf{p}_B - \mathbf{p}'_B = \tilde{\mathbf{p}}_B - \tilde{\mathbf{p}}'_B$ can be expressed by their coordinates relative to the orthogonal basis of unit vectors $\hat{\mathbf{x}}, \hat{\mathbf{y}}$, and $\hat{\mathbf{z}}$ along the axes x, y and z (see Fig. 5):

$$\tilde{\mathbf{p}}_B = \tilde{p}_B \begin{pmatrix} 0 \\ 0 \\ 1 \end{pmatrix}, \quad \tilde{\mathbf{p}}'_B = \tilde{p}_B \begin{pmatrix} -\sin \alpha \cos \phi \\ -\sin \alpha \sin \phi \\ -\cos \alpha \end{pmatrix}, \quad \mathbf{q}_B = \tilde{p}_B \begin{pmatrix} \sin \alpha \cos \phi \\ \sin \alpha \sin \phi \\ 1 + \cos \alpha \end{pmatrix} \quad (26)$$

where $\tilde{p}_B = \mu |\mathbf{v}_B - \mathbf{v}_S|$, with $\mu = (m_B^{-1} + m_S^{-1})^{-1}$.

Let $f(\mathbf{v}_S)$ be the one-particle probability distribution function of S -particles S . In terms of $f(\mathbf{v}_S)$, the ensemble-averaged momentum lost by the particle B during δt reads:

$$\begin{aligned} \langle \mathbf{q}_B \rangle &= \iiint f(\mathbf{v}_S) d^3 \mathbf{v}_S \iint \mu |\mathbf{v}_B - \mathbf{v}_S| \begin{pmatrix} \sin \alpha \cos \phi \\ \sin \alpha \sin \phi \\ 1 + \cos \alpha \end{pmatrix} d^2 N \\ &= n_S \mu \left(\frac{R_B + R_S}{2}\right)^2 \delta t \iiint f(\mathbf{v}_S) d^3 \mathbf{v}_S \int_{-\pi}^{+\pi} \int_0^\pi |\mathbf{v}_B - \mathbf{v}_S|^2 \begin{pmatrix} \sin \alpha \cos \phi \\ \sin \alpha \sin \phi \\ 1 + \cos \alpha \end{pmatrix} \sin \alpha d\alpha d\phi \end{aligned}$$

$$\begin{aligned}
&= 4\pi n_S \mu \left(\frac{R_B + R_S}{2} \right)^2 \delta t \iiint f(\mathbf{v}_S) |\mathbf{v}_B - \mathbf{v}_S|^2 \begin{pmatrix} 0 \\ 0 \\ 1 \end{pmatrix} d^3 \mathbf{v}_S \\
&= 4\pi n_S \mu \left(\frac{R_B + R_S}{2} \right)^2 \delta t \iiint f(\mathbf{v}_S) |\mathbf{v}_B - \mathbf{v}_S| (\mathbf{v}_B - \mathbf{v}_S) d^3 \mathbf{v}_S.
\end{aligned} \tag{27}$$

If the surrounding gas is sufficiently diluted, the distribution function $f(\mathbf{v}_S)$ can be modelled by the stationary solution of Boltzmann's equation in the presence of a uniform thermal gradient:

$$f(\mathbf{v}_S) = \left(\frac{2\pi k_B T}{m_S} \right)^{-\frac{3}{2}} \exp\left(-\frac{m_S v_S^2}{2k_B T}\right) \left\{ 1 - \left(\frac{m_S v_S^2}{2k_B T} - \frac{5}{2} \right) \frac{3\nu_S(T)m_S}{2k_B T} \mathbf{v}_S \cdot \frac{\nabla T}{T} \right\}, \tag{28}$$

where $k_B T$ is the Boltzmann factor, and $\nu_S(T)$ is the kinematic shear viscosity of the surrounding gas:

$$\nu_S(T) = \frac{5\sqrt{\pi}}{16} \frac{1}{n_S \pi (2R_S)^2} \sqrt{\frac{k_B T}{m_S}}. \tag{29}$$

Let us now introduce the thermal velocity $\sqrt{k_B T/m_S}$ of the gas particles. The dimensionless velocity variables \mathbf{u}_B , \mathbf{u}_S and \mathbf{w} are defined as follows:

$$\mathbf{u}_B = \sqrt{\frac{m_S}{k_B T}} \mathbf{v}_B \quad \text{and} \quad \mathbf{u}_S = \sqrt{\frac{m_S}{k_B T}} \mathbf{v}_S \quad \text{and} \quad \mathbf{w} = \mathbf{u}_S - \mathbf{u}_B. \tag{30}$$

We also need to introduce the unit vector $\mathbf{g} = \nabla T / |\nabla T|$ lying along the direction of the thermal gradient. The averaged momentum loss then reads:

$$\langle \mathbf{q}_B \rangle = -A_1 (\mathcal{I}_1(u_B) - B \mathcal{I}_2(u_B)), \tag{31}$$

where the coefficients A_1 and B are:

$$A_1 = \sqrt{\frac{2}{\pi}} \mu n_S \delta t \left(\frac{R_B + R_S}{2} \right)^2 \frac{k_B T}{m_S} \quad \text{and} \quad B = \frac{3\nu_S(T)}{4} \sqrt{\frac{m_S}{k_B T}} \left| \frac{\nabla T}{T} \right|, \tag{32}$$

and where the integrals $\mathcal{I}_1(u_B)$ and $\mathcal{I}_2(u_B)$ are:

$$\begin{aligned}
\mathcal{I}_1(\mathbf{u}_B) &= \iiint e^{-\frac{(\mathbf{w} + \mathbf{u}_B)^2}{2}} |\mathbf{w}| \mathbf{w} d^3 \mathbf{w}, \\
\mathcal{I}_2(\mathbf{u}_B) &= \iiint e^{-\frac{(\mathbf{w} + \mathbf{u}_B)^2}{2}} (|\mathbf{w} + \mathbf{u}_B|^2 - 5) (\mathbf{w} + \mathbf{u}_B) \cdot \mathbf{g} |\mathbf{w}| \mathbf{w} d^3 \mathbf{w}.
\end{aligned} \tag{33}$$

A new set of reference axes X , Y and Z is needed to compute these integrals (see Fig. 7). The Z axis lies along the velocity \mathbf{v}_B of the Brownian particle. The X axis is orthogonal to the Z axis, and such that the thermal gradient ∇T lies in the plane (XZ) . With respect to this new set of axes, the components of the dimensionless relative velocity \mathbf{w} and of the unit vector \mathbf{g} along which lies the temperature gradient are:

$$\mathbf{w} = w \begin{pmatrix} \sin \gamma \cos \psi \\ \sin \gamma \sin \psi \\ \cos \gamma \end{pmatrix} \quad \text{and} \quad \mathbf{g} = \begin{pmatrix} \sin \Omega \\ 0 \\ \cos \Omega \end{pmatrix}, \tag{34}$$

where $w = |\mathbf{w}|$.

Let us first compute \mathcal{I}_1 :

$$\begin{aligned}
\mathcal{I}_1(\mathbf{u}_B) &= \int_0^{+\infty} e^{-\frac{(w^2 + u_B^2)}{2}} w^4 \int_0^\pi e^{-u_B w \cos \gamma} \int_{-\pi}^{+\pi} \begin{pmatrix} \sin \gamma \cos \psi \\ \sin \gamma \sin \psi \\ \cos \gamma \end{pmatrix} d\psi \sin \gamma d\gamma dw \\
&= 2\pi \int_0^{+\infty} e^{-\frac{(w^2 + u_B^2)}{2}} w^4 \int_{-1}^1 e^{-u_B w \lambda} \begin{pmatrix} 0 \\ 0 \\ 1 \end{pmatrix} \lambda d\lambda dw \\
&= 2F_4^1(u_B) \frac{\mathbf{u}_B}{u_B},
\end{aligned} \tag{35}$$

where $u_B = |\mathbf{u}_B|$, and where the family of functions $F_k^l(u)$, for $l \geq 0$ and $k > l$ is defined by:

$$F_k^l(u) = \pi \int_0^{+\infty} e^{-\frac{(w^2 + u^2)}{2}} w^k \int_{-1}^1 e^{-uw\lambda} \lambda^l d\lambda dw. \tag{36}$$

All these functions can be explicitly computed. Appendix B is dedicated to these calculations.

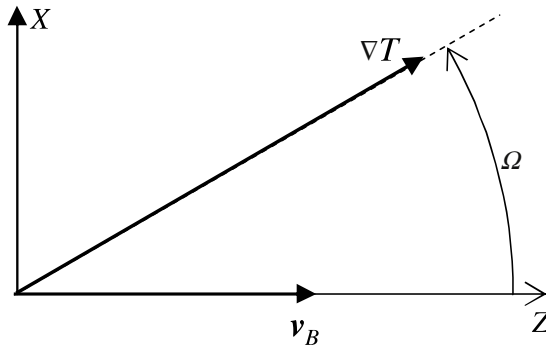


Fig. 7. Definition of the axes X, Y and Z. The axis Z is along the velocity of the Brownian particle. The axis X is defined so that the temperature gradient lies in the (XZ) plane, and Y is such that (X, Y, Z) is a positive set of orthogonal axes.

A similar computation leads to:

$$\begin{aligned}
 \mathcal{I}_2(\mathbf{u}_B) = & ((u_B^2 - 5)(F_5^0 - F_5^2) + 2u_B(F_6^1 - F_6^3) + F_7^0 - F_7^2) \mathbf{g} \\
 & + (2u_B(u_B^2 - 5)F_4^1 - (u_B^2 - 5)F_5^0 + (7u_B^2 - 15)F_5^2 + 6u_B F_6^3 - F_7^0 + 3F_7^2) \cos \Omega \frac{\mathbf{u}_B}{u_B},
 \end{aligned} \tag{37}$$

where F_k^l is short for $F_k^l(u_B)$.

Gathering the results in (35) and (37), we obtain the desired expression for the averaged momentum loss:

$$\begin{aligned}
 \langle \mathbf{q}_B \rangle(\mathbf{u}_B) = & \left\{ -2F_4^1 + \left(2u_B(u_B^2 - 5)F_4^1 - (u_B^2 - 5)F_5^0 + (7u_B^2 - 15)F_5^2 + 6u_B F_6^3 - F_7^0 + 3F_7^2 \right) B \cos \Omega \right\} A_1 \frac{\mathbf{u}_B}{u_B} \\
 & + \left\{ (u_B^2 - 5)(F_5^0 - F_5^2) + 2u_B(F_6^1 - F_6^3) + F_7^0 - F_7^2 \right\} A_1 B \mathbf{g}.
 \end{aligned} \tag{38}$$

The term proportional to \mathbf{g} , and thus to ∇T leads to the thermophoresis force. The term proportional to \mathbf{u}_B leads to the friction force, with a contribution independent of the temperature gradient, and a correction proportional to the projection of the temperature gradient onto the velocity of the Brownian particle.

To obtain self-contained analytical expressions of $\langle \mathbf{q}_B \rangle(\mathbf{u}_B)$, one needs the expressions of the $F_k^l(x)$ functions (see Appendix B). These lead to:

$$\begin{aligned}
 \langle \mathbf{q}_B \rangle(\mathbf{u}_B) = & 2\pi \left(\frac{-2 + 4u_B^2 + 2u_B^4}{u_B^2} \zeta(u_B) + \frac{2 + 2u_B^2}{u_B^2} \xi(u_B) \right) A_1 \mathbf{u}_B \\
 & + 2\pi \left(\frac{24 - 8u_B^2}{u_B^4} \zeta(u_B) - \frac{24}{u_B^4} \xi(u_B) \right) B u_B \cos \Omega A_1 \mathbf{u}_B \\
 & + 2\pi \left(\frac{-8 + 8u_B^2}{u_B^2} \zeta(u_B) + \frac{8}{u_B^2} \xi(u_B) \right) A_1 B \mathbf{g}
 \end{aligned} \tag{39}$$

where the functions $\zeta(u_B)$ and $\xi(u_B)$ are defined as:

$$\zeta(u_B) \equiv \sqrt{\frac{2}{\pi}} \frac{\text{erf}(u_B/\sqrt{2})}{u_B} \quad \text{and} \quad \xi(u_B) \equiv e^{-\frac{u_B^2}{2}}. \tag{40}$$

Taking into account de value (32) of A_1 and B , one ends up with:

$$\begin{aligned}
 \frac{\langle \mathbf{q}_B \rangle(\mathbf{u}_B)}{\delta t} = & \sqrt{2\pi} n_S \mu (R_B + R_S)^2 \frac{k_B T}{m_S} \left\{ \left(\frac{-1 + 2u_B^2 + u_B^4}{u_B^2} \zeta(u_B) + \frac{1 + u_B^2}{u_B^2} \xi(u_B) \right) \mathbf{u}_B \right. \\
 & + \left(\frac{3 - u_B^2}{u_B^4} \zeta(u_B) - \frac{3}{u_B^4} \xi(u_B) \right) 3v_S(T) \sqrt{\frac{m_S}{k_B T}} \left(\mathbf{u}_B \cdot \frac{\nabla T}{T} \right) \mathbf{u}_B \\
 & \left. + \left(\frac{-1 + u_B^2}{u_B^2} \zeta(u_B) + \frac{1}{u_B^2} \xi(u_B) \right) 3v_S(T) \sqrt{\frac{m_S}{k_B T}} \frac{\nabla T}{T} \right\}.
 \end{aligned} \tag{41}$$

Since \mathbf{u}_B is the ratio of the Brownian particle's velocity \mathbf{v}_B to the thermal velocity of the gas particles (see Eq. (30)), the case of small values of u_B is of particular physical interest. In this limit case, the following expansion can be used:

$$\langle \mathbf{q}_B \rangle(\mathbf{u}_B) = 2\pi \left\{ \left(\frac{16}{3} + \frac{8}{15} u_B^2 \right) + \left(-\frac{16}{15} + \frac{8}{35} u_B^2 \right) B u_B \cos \Omega \right\} A_1 \mathbf{u}_B + 2\pi \left\{ \frac{16}{3} - \frac{8}{15} u_B^2 \right\} A_1 B \mathbf{g} + \mathcal{O}(u_B^4), \tag{42}$$

which leads to the following expression in terms of the physically relevant parameters:

$$\begin{aligned} \frac{\langle \mathbf{q}_B \rangle (\mathbf{u}_B)}{\delta t} &= \sqrt{2\pi} n_S \mu (R_B + R_S)^2 \frac{k_B T}{m_S} \left\{ \left(\left(\frac{8}{3} + \frac{4}{15} u_B^2 \right) + \left(-\frac{2}{15} + \frac{1}{35} u_B^2 \right) 3\nu_S(T) \sqrt{\frac{m_S}{k_B T}} \left(\mathbf{u}_B \cdot \frac{\nabla T}{T} \right) \right) \mathbf{u}_B \right. \\ &\quad \left. + \left(\frac{2}{3} - \frac{1}{15} u_B^2 \right) 3\nu_S(T) \sqrt{\frac{m_S}{k_B T}} \frac{\nabla T}{T} \right\} + \mathcal{O}(u_B^4). \end{aligned} \quad (43)$$

A.3. Computation of the expectation $\langle \mathbf{q}_B \otimes \mathbf{q}_B \rangle$

The computation of the ensemble-averaged squared momentum loss tensor $\langle \mathbf{q}_B \otimes \mathbf{q}_B \rangle$ follows the same guidelines as the computation of $\langle \mathbf{q}_B \rangle$ developed in [Appendix A.2](#):

$$\begin{aligned} \langle \mathbf{q}_B \otimes \mathbf{q}_B \rangle &= \iint f(\mathbf{v}_S) d^3 \mathbf{v}_S \iint \mu^2 |\mathbf{v}_B - \mathbf{v}_S|^2 \begin{pmatrix} \sin \alpha \cos \phi \\ \sin \alpha \sin \phi \\ 1 + \cos \alpha \end{pmatrix} \otimes \begin{pmatrix} \sin \alpha \cos \phi \\ \sin \alpha \sin \phi \\ 1 + \cos \alpha \end{pmatrix} d^2 N \\ &= n_S \mu^2 \left(\frac{R_B + R_S}{2} \right)^2 \delta t \iint f(\mathbf{v}_S) d^3 \mathbf{v}_S \int_{-\pi}^{+\pi} \int_0^\pi |\mathbf{v}_B - \mathbf{v}_S|^3 \\ &\quad \times \begin{pmatrix} \sin^2 \alpha \cos^2 \phi & \sin^2 \alpha \sin \phi \cos \phi & \sin \alpha (1 + \cos \alpha) \cos \phi \\ \sin^2 \alpha \sin \phi \cos \phi & \sin^2 \alpha \sin^2 \phi & \sin \alpha (1 + \cos \alpha) \sin \phi \\ \sin \alpha (1 + \cos \alpha) \cos \phi & \sin \alpha (1 + \cos \alpha) \sin \phi & (1 + \cos \alpha)^2 \end{pmatrix} \sin \alpha d\alpha d\phi \\ &= \frac{4\pi}{3} n_S \mu^2 \left(\frac{R_B + R_S}{2} \right)^2 \delta t \iint f(\mathbf{v}_S) |\mathbf{v}_B - \mathbf{v}_S|^3 \begin{pmatrix} 1 & 0 & 0 \\ 0 & 1 & 0 \\ 0 & 0 & 4 \end{pmatrix} d^3 \mathbf{v}_S \\ &= \frac{4\pi}{3} n_S \mu^2 \left(\frac{R_B + R_S}{2} \right)^2 \delta t \iint f(\mathbf{v}_S) |\mathbf{v}_B - \mathbf{v}_S| (|\mathbf{v}_B - \mathbf{v}_S|^2 \mathcal{E} + 3(\mathbf{v}_B - \mathbf{v}_S) \otimes (\mathbf{v}_B - \mathbf{v}_S)) d^3 \mathbf{v}_S, \end{aligned} \quad (44)$$

where \mathcal{E} denotes the unit tensor. As in [Appendix A.2](#), the expression for the averaged squared momentum loss tensor splits into two integrals:

$$\langle \mathbf{q}_B \otimes \mathbf{q}_B \rangle = A_2 (\mathcal{I}_3(u_B) - B \mathcal{I}_4(u_B)), \quad (45)$$

where the coefficients A_2 and B are:

$$A_2 = \frac{1}{3} \sqrt{\frac{2}{\pi}} \mu^2 n_S \delta t \left(\frac{R_B + R_S}{2} \right)^2 \left(\frac{k_B T}{m_S} \right)^{\frac{3}{2}} \quad \text{and} \quad B = \frac{3\nu_S(T)}{4} \sqrt{\frac{m_S}{k_B T}} \left| \frac{\nabla T}{T} \right|, \quad (46)$$

and where the integrals $\mathcal{I}_3(u_B)$ and $\mathcal{I}_4(u_B)$ are:

$$\begin{aligned} \mathcal{I}_3(\mathbf{u}_B) &= \iiint e^{-\frac{(\mathbf{w} + \mathbf{u}_B)^2}{2}} |\mathbf{w}| (|\mathbf{w}|^2 \mathcal{E} + 3\mathbf{w} \otimes \mathbf{w}) d^3 \mathbf{w}, \\ \mathcal{I}_4(\mathbf{u}_B) &= \iiint e^{-\frac{(\mathbf{w} + \mathbf{u}_B)^2}{2}} (|\mathbf{w} + \mathbf{u}_B|^2 - 5) (\mathbf{w} + \mathbf{u}_B) \cdot \mathbf{g} |\mathbf{w}| (|\mathbf{w}|^2 \mathcal{E} + 3\mathbf{w} \otimes \mathbf{w}) d^3 \mathbf{w}. \end{aligned} \quad (47)$$

We use again the reference axes X , Y and Z defined in [Appendix A.2](#) and in [Fig. 7](#). On this new basis, the components of the tensor $(|\mathbf{w}|^2 \mathcal{E} + 3\mathbf{w} \otimes \mathbf{w})$ are:

$$(|\mathbf{w}|^2 \mathcal{E} + 3\mathbf{w} \otimes \mathbf{w}) = w^2 \begin{pmatrix} 1 + 3 \sin^2 \gamma \cos^2 \psi & 3 \sin^2 \gamma \sin \psi \cos \psi & 3 \sin \gamma \cos \gamma \cos \psi \\ 3 \sin^2 \gamma \sin \psi \cos \psi & 1 + 3 \sin^2 \gamma \sin^2 \psi & 3 \sin \gamma \cos \gamma \sin \psi \\ 3 \sin \gamma \cos \gamma \cos \psi & 3 \sin \gamma \cos \gamma \sin \psi & 1 + 3 \cos^2 \gamma \end{pmatrix} \quad (48)$$

where $w = |\mathbf{w}|$. A straightforward computation leads to:

$$\mathcal{I}_3(\mathbf{u}_B) = \begin{pmatrix} 5F_5^0 - 3F_5^3 & 0 & 0 \\ 0 & 5F_5^0 - 3F_5^3 & 0 \\ 0 & 0 & 2F_5^0 + 6F_5^3 \end{pmatrix} \quad (49)$$

where the family of functions F_k^l has already been defined by [Eq. \(36\)](#) and, as before, F_k^l is short for $F_k^l(\mathbf{u}_B)$. The tensor $\mathcal{I}_3(\mathbf{u}_B)$ can be expressed as a linear combination of \mathcal{E} and of $\mathbf{u}_B \otimes \mathbf{u}_B$ as follows:

$$\mathcal{I}_3(\mathbf{u}_B) = (5F_5^0 - 3F_5^3) \mathcal{E} - 3(F_5^0 - 3F_5^3) \frac{\mathbf{u}_B \otimes \mathbf{u}_B}{u_B^2}. \quad (50)$$

One also finds by direct computation that

$$\mathcal{I}_4(\mathbf{u}_B) = \begin{pmatrix} I_4^{11}(u_B) & 0 & I_4^{13}(u_B) \\ 0 & I_4^{22}(u_B) & 0 \\ I_4^{31}(u_B) & 0 & I_4^{33}(u_B) \end{pmatrix}, \tag{51}$$

where the components $I_4^{11}(u_B)$, $I_4^{22}(u_B)$, $I_4^{33}(u_B)$, $I_4^{13}(u_B)$ and $I_4^{31}(u_B)$ are given by:

$$I_4^{11}(u_B) = I_4^{22}(u_B) = \cos \Omega \left(u_B(u_B^2 - 5)(5F_5^0 - 3F_5^2) + (3u_B^2 - 5)(5F_6^1 - 3F_6^3) + u_B(5F_7^0 + 7F_7^2 - 6F_7^4) + (5F_8^1 - 3F_8^3) \right), \tag{52}$$

$$I_4^{33}(u_B) = 2 \cos \Omega \left(u_B(u_B^2 - 5)(F_5^0 + 3F_5^2) + (3u_B^2 - 5)(F_6^1 + 3F_6^3) + u_B(F_7^0 + 5F_7^2 + 6F_7^4) + (F_8^1 + 3F_8^3) \right), \tag{53}$$

and

$$I_4^{13}(u_B) = I_4^{31}(u_B) = 3 \sin \Omega \left((u_B^2 - 5)(F_6^1 - F_6^3) + 2u_B(F_7^2 - F_7^4) + (F_8^1 - F_8^3) \right). \tag{54}$$

The tensor $\mathcal{I}_4(\mathbf{u}_B)$ can be expressed as a linear combination of the three tensors \mathcal{E} , $\mathbf{u}_B \otimes \mathbf{u}_B$ and $\mathbf{u}_B \otimes \mathbf{g} + \mathbf{g} \otimes \mathbf{u}_B$ as follows:

$$\mathcal{I}_4(\mathbf{u}_B) = I_4^{11}(u_B)\mathcal{E} + \left(I_4^{33}(u_B) - I_4^{11}(u_B) - 2 \frac{\cos \Omega}{\sin \Omega} I_4^{13}(u_B) \right) \frac{\mathbf{u}_B \otimes \mathbf{u}_B}{u_B^2} + \frac{I_4^{13}(u_B)}{\sin \Omega} \frac{\mathbf{u}_B \otimes \mathbf{g} + \mathbf{g} \otimes \mathbf{u}_B}{u_B}. \tag{55}$$

Thus, the averaged squared momentum loss tensor reads:

$$\begin{aligned} \langle \mathbf{q}_B \otimes \mathbf{q}_B \rangle(\mathbf{u}_B) &= \left\{ (5F_5^0 - 3F_5^2) - \left(u_B(u_B^2 - 5)(5F_5^0 - 3F_5^2) + (3u_B^2 - 5)(5F_6^1 - 3F_6^3) \right. \right. \\ &\quad \left. \left. + u_B(5F_7^0 + 7F_7^2 - 6F_7^4) + 5F_8^1 - 3F_8^3 \right) B \cos \Omega \right\} A_2 \mathcal{E} \\ &- 3 \left\{ (F_5^0 - 3F_5^2) + \left(u_B(u_B^2 - 5)(F_5^0 - 3F_5^2) + (5u_B^2 - 15)F_6^1 \right. \right. \\ &\quad \left. \left. - (11u_B^2 - 25)F_6^3 + u_B(F_7^0 + 3F_7^2 - 10F_7^4) + 3F_8^1 - 5F_8^3 \right) B \cos \Omega \right\} A_2 \frac{\mathbf{u}_B \otimes \mathbf{u}_B}{u_B^2} \\ &- 3 \left\{ (u_B^2 - 5)(5F_6^1 - F_6^3) + 2u_B(F_7^2 - F_7^4) + F_8^1 - F_8^3 \right\} BA_2 \frac{\mathbf{u}_B \otimes \mathbf{g} + \mathbf{g} \otimes \mathbf{u}_B}{u_B}. \end{aligned} \tag{56}$$

To obtain self-contained analytical expressions of $\langle \mathbf{q}_B \otimes \mathbf{q}_B \rangle(\mathbf{u}_B)$, one needs the expressions of the F_k^l functions (see Appendix B). This leads to:

$$\begin{aligned} \langle \mathbf{q}_B \otimes \mathbf{q}_B \rangle(\mathbf{u}_B) &= 2\pi \left(\frac{-6 + 18u_B^2 + 18u_B^4 + 2u_B^6}{u_B^2} \zeta(u_B) + \frac{6 + 16u_B^2 + 2u_B^4}{u_B^2} \xi(u_B) \right) A_2 \mathcal{E} \\ &+ 2\pi \left(\frac{108 - 72u_B^2 + 36u_B^4}{u_B^4} \zeta(u_B) + \frac{-108 + 36u_B^2}{u_B^4} \xi(u_B) \right) Bu_B \cos \Omega A_2 \mathcal{E} \\ &+ 2\pi \left(\frac{18 - 18u_B^2 + 18u_B^4 + 6u_B^6}{u_B^4} \zeta(u_B) + \frac{-18 + 12u_B^2 + 6u_B^4}{u_B^4} \xi(u_B) \right) A_2 \mathbf{u}_B \otimes \mathbf{u}_B \\ &+ 2\pi \left(\frac{540 - 216u_B^2 + 36u_B^4}{u_B^6} \zeta(u_B) + \frac{-540 + 36u_B^2}{u_B^6} \xi(u_B) \right) Bu_B \cos \Omega A_2 \mathbf{u}_B \otimes \mathbf{u}_B \\ &+ 2\pi \left(\frac{108 + 108u_B^2 - 540u_B^4 - 432u_B^6 + 48u_B^8 + 12u_B^{10}}{u_B^4} \zeta(u_B) \right. \\ &\quad \left. + \frac{-108 - 144u_B^2 - 444u_B^4 + 36u_B^6 + 12u_B^8}{u_B^4} \xi(u_B) \right) A_2 B(\mathbf{u}_B \otimes \mathbf{g} + \mathbf{g} \otimes \mathbf{u}_B) \end{aligned} \tag{57}$$

where the functions $\zeta(u_B)$ and $\xi(u_B)$ have been defined by (40). Taking into account de value (46) of A_2 and B , one ends up with:

$$\begin{aligned} \frac{\langle \mathbf{q}_B \otimes \mathbf{q}_B \rangle(\mathbf{u}_B)}{2\delta t} &= \frac{1}{6} \sqrt{2\pi} n_S \mu^2 (R_B + R_S)^2 \left(\frac{k_B T}{m_S}\right)^{\frac{3}{2}} \left\{ \left(\frac{-3 + 9u_B^2 + 9u_B^4 + u_B^6}{u_B^2} \zeta(u_B) + \frac{3 + 8u_B^2 + u_B^4}{u_B^2} \xi(u_B) \right) \mathcal{E} \right. \\ &+ \left(\frac{3 - 2u_B^2 + u_B^4}{u_B^4} \zeta(u_B) + \frac{-3 + u_B^2}{u_B^4} \xi(u_B) \right) \frac{27}{2} \nu_S(T) \sqrt{\frac{m_S}{k_B T}} \left(\mathbf{u}_B \cdot \frac{\nabla T}{T} \right) \mathcal{E} \\ &+ \left(\frac{3 - 3u_B^2 + 3u_B^4 + u_B^6}{u_B^4} \zeta(u_B) + \frac{-3 + 2u_B^2 + u_B^4}{u_B^4} \xi(u_B) \right) 3\mathbf{u}_B \otimes \mathbf{u}_B \\ &+ \left(\frac{15 - 6u_B^2 + u_B^4}{u_B^6} \zeta(u_B) + \frac{-15 + u_B^2}{u_B^6} \xi(u_B) \right) \frac{27}{2} \nu_S(T) \sqrt{\frac{m_S}{k_B T}} \left(\mathbf{u}_B \cdot \frac{\nabla T}{T} \right) \mathbf{u}_B \otimes \mathbf{u}_B \\ &+ \left(\frac{9 + 9u_B^2 - 45u_B^4 - 36u_B^6 + 4u_B^8 + u_B^{10}}{u_B^4} \zeta(u_B) \right. \\ &\left. + \frac{-9 - 12u_B^2 - 37u_B^4 + 3u_B^6 + u_B^8}{u_B^4} \xi(u_B) \right) 9\nu_S(T) \sqrt{\frac{m_S}{k_B T}} \frac{\mathbf{u}_B \otimes \nabla T + \nabla T \otimes \mathbf{u}_B}{2T} \left. \right\}. \end{aligned} \tag{58}$$

Expanding $\langle \mathbf{q}_B \otimes \mathbf{q}_B \rangle(\mathbf{u}_B)$ in u_B , one gets:

$$\begin{aligned} \langle \mathbf{q}_B \otimes \mathbf{q}_B \rangle(\mathbf{u}_B) &= 2\pi \left\{ \left(32 + \frac{48}{5} u_B^2 \right) + \left(\frac{96}{5} - \frac{48}{35} u_B^2 \right) B u_B \cos \Omega \right\} A_2 \mathcal{E} \\ &+ 2\pi \left\{ \left(\frac{96}{5} + \frac{48}{35} u_B^2 \right) + \left(\frac{96}{35} - \frac{16}{35} u_B^2 \right) B u_B \cos \Omega \right\} A_2 \mathbf{u}_B \otimes \mathbf{u}_B \\ &+ 2\pi \left\{ -\frac{4704}{5} - \frac{3408}{35} u_B^2 \right\} A_2 B (\mathbf{u}_B \otimes \mathbf{g} + \mathbf{g} \otimes \mathbf{u}_B) + \mathcal{O}(u_B^4) \end{aligned} \tag{59}$$

which leads to the following expression in terms of the physically relevant parameters:

$$\begin{aligned} \frac{\langle \mathbf{q}_B \otimes \mathbf{q}_B \rangle(\mathbf{u}_B)}{2\delta t} &= \frac{1}{6} \sqrt{2\pi} \left(\frac{m_B}{m_B + m_S} \right)^2 (R_B + R_S)^2 n_S \sqrt{k_B T m_S k_B T} \left\{ \left(\left(16 + \frac{24}{5} u_B^2 \right) \right. \right. \\ &+ \left. \left(\frac{12}{5} - \frac{6}{35} u_B^2 \right) 3\nu_S(T) \sqrt{\frac{m_S}{k_B T}} \left(\mathbf{u}_B \cdot \frac{\nabla T}{T} \right) \right) \mathcal{E} \\ &+ \left(\left(\frac{48}{5} + \frac{24}{35} u_B^2 \right) + \left(\frac{12}{35} - \frac{2}{35} u_B^2 \right) 3\nu_S(T) \sqrt{\frac{m_S}{k_B T}} \left(\mathbf{u}_B \cdot \frac{\nabla T}{T} \right) \right) \mathbf{u}_B \otimes \mathbf{u}_B \\ &+ \left. \left(-\frac{1176}{5} - \frac{852}{35} u_B^2 \right) 3\nu_S(T) \sqrt{\frac{m_S}{k_B T}} \frac{\mathbf{u}_B \otimes \nabla T + \nabla T \otimes \mathbf{u}_B}{2T} \right\} + \mathcal{O}(u_B^4). \end{aligned} \tag{60}$$

Appendix B. Computation of the F_k^l functions

In Appendix A.2, the functions F_k^l were introduced to make algebraic expressions more tractable. These functions were defined by Eq. (36), which we here recall:

$$F_k^l(x) = \pi \int_0^{+\infty} e^{-\frac{(w^2+x^2)}{2}} w^k \int_{-1}^1 e^{-xw\lambda} \lambda^l d\lambda dw. \tag{61}$$

This definition holds for all integers k and l , $0 \leq l < k$, and real x . The members to be computed are: $F_4^1, F_5^0, F_5^2, F_6^1, F_6^3, F_7^0, F_7^2, F_7^4, F_8^1$, and F_8^3 .

A simple strategy to compute explicit expressions for these functions, is (i) to compute F_3^0, F_5^0 , and F_7^0 as explained below, and (ii) to use the recurrence relation:

$$F_{k+1}^{l+1}(x) = -xF_k^l(x) - \frac{d}{dx} F_k^l(x) \tag{62}$$

to compute successively $F_4^1, F_5^2, F_6^3, F_7^4$ from F_3^0 , then F_6^1, F_7^2, F_8^3 from F_5^0 , then finally F_8^1 from F_7^0 . Fig. 8 shows a diagram in (k, l) space, where all these required F_k^l 's are displayed as solid disks. F_3^0, F_5^0 , and F_7^0 are displayed as squares. The arrow shows the effect of the recurrence formula (62).

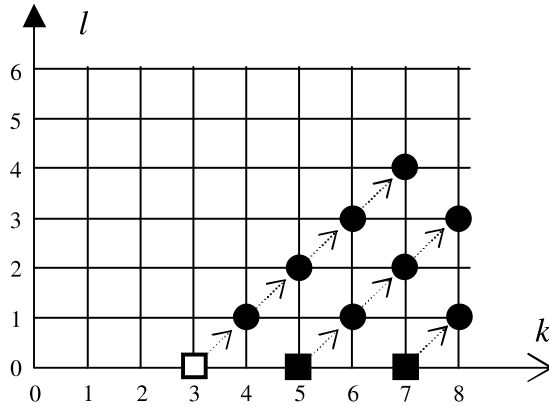


Fig. 8. Diagram showing in the (k, l) space which F_k^l 's are needed to compute $\langle \mathbf{q} \rangle$ and $\langle \mathbf{q} \otimes \mathbf{q} \rangle$. Solid symbols represent needed values of (k, l) . Square symbols designate values of k such that F_k^0 is needed as a starting point of the recurrence process leading to all other required F_k^l 's. The arrows show the action of the recurrence formula (62).

To compute F_k^0 for $k > 0$, we need to introduce the family of functions $\Lambda_k(x)$ defined by:

$$\Lambda_k(x) = \int_0^{+\infty} e^{-\frac{(w+x)^2}{2}} w^k dw. \tag{63}$$

In terms of the Λ_k 's, the F_k^0 's read:

$$F_{k+1}^0(x) = \frac{\pi}{x} (\Lambda_k(-x) - \Lambda_k(x)), \quad \text{for } k \geq 0. \tag{64}$$

It can be noticed that the Λ_k 's can be expressed as follows:

$$\Lambda_k(x) = P_k(x)e^{-\frac{x^2}{2}} + Q_k(x)\sqrt{\frac{\pi}{2}} \left(1 - \operatorname{erf}\left(\frac{x}{\sqrt{2}}\right) \right), \tag{65}$$

where $P_k(x)$ and $Q_k(x)$ for $k \geq 0$ are two families of polynomials of degree $k - 1$ and k respectively, which can be computed according to the following recursive procedure:

$$\begin{cases} P_0(x) = 0 \\ Q_0(x) = 1 \end{cases} \quad \text{and} \quad \begin{cases} P_{i+1}(x) = Q_i(x) - \frac{d}{dx}P_i(x) \\ Q_{i+1}(x) = -xQ_i(x) - \frac{d}{dx}Q_i(x). \end{cases} \tag{66}$$

The first members of these families are thus:

$$\begin{array}{ll} P_0(x) = 0 & Q_0(x) = 1 \\ P_1(x) = 1 & Q_1(x) = -x \\ P_2(x) = -x & Q_2(x) = 1 + x^2 \\ P_3(x) = 2 + x^2 & Q_3(x) = -3x - x^3 \\ P_4(x) = -5x - x^3 & Q_4(x) = 3 + 6x^2 + x^4 \\ P_5(x) = 8 + 9x^2 + x^4 & Q_5(x) = -15x - 10x^3 - x^5 \\ P_6(x) = -33x - 14x^3 - x^5 & Q_6(x) = 15 + 45x^2 + 15x^4 + x^6. \end{array} \tag{67}$$

When k is even, Q_k is even and P_k is odd. When k is odd, Q_k is odd and P_k is even:

$$\begin{aligned} P_{2j}(-x) &= -P_{2j}(x), & Q_{2j}(-x) &= Q_{2j}(x), \\ P_{2j+1}(-x) &= P_{2j+1}(x), & Q_{2j+1}(-x) &= -Q_{2j+1}(x). \end{aligned} \tag{68}$$

Thus, using (64) and (65), a compact expression of the F_k^0 's can be derived:

$$\begin{cases} F_{2j+1}^0(x) = 2\pi \left(-\frac{P_{2j}(x)}{x} e^{-\frac{x^2}{2}} + \frac{Q_{2j}(x)}{x} \sqrt{\frac{\pi}{2}} \operatorname{erf}\left(\frac{x}{\sqrt{2}}\right) \right), \\ F_{2j+2}^0(x) = -\pi \sqrt{2\pi} \frac{Q_{2j+1}(x)}{x} \end{cases} \quad \text{for } j \geq 0. \tag{69}$$

References

- [1] J. Luettmmer-Strathmann, Two-chamber lattice model for thermodiffusion in polymer solutions, *J. Chem. Phys.* 119 (5) (2003) 2892–2902.
- [2] S. Duhr, S. Arduini, D. Braun, Thermophoresis of DNA determined by microfluidic fluorescence, *Appl. Phys. Lett.* 15 (2004) 277–286.
- [3] S. Duhr, D. Braun, Two-dimensional colloidal crystals formed by thermophoresis and convection, *Appl. Phys. Lett.* 86 (2005) 131921.
- [4] Z. Dashevsky, V. Kasiyan, E. Mogilko, A. Butenko, R. Kahatabi, S. Genikov, V. Sandomirsky, Y. Schlesinger, High-temperature PbTe diodes, 2007. arXiv:0707.1213.
- [5] <http://www.ulb.ac.be/polytech/mrc/PDFFiles/DSC.pdf>.
- [6] L.D. Landau, E.M. Lifschitz, *Fluid Mechanics*, 2nd ed., Pergamon Press, 1987.
- [7] A. Einstein, *Investigations on the theory of the Brownian movement*, Ph.D. Thesis, Dover, 1956.
- [8] N.G. van Kampen, *Stochastic Processes in Physics and Chemistry*, 3rd ed., Elsevier, 2007.
- [9] N.G. van Kampen, *IBM J. Res. Dev.* 32 (1988) 107.
- [10] M.E. Widder, U.M. Titulaer, *Physica A* 154 (1989) 452.
- [11] E. Bringuier, A. Bourdon, *Physica A* 385 (2007) 9.
- [12] S.Q. Ma, *Statistical Mechanics*, World Scientific, 1985.
- [13] C. Chevalier, F. Debbasch, J.P. Rivet, A stochastic approach to thermodiffusion, in: Proc. to IFHT08, Heat Transfer Society of Japan, 2008.
- [14] C. Chevalier, F. Debbasch, J.P. Rivet, Stochastic models of thermodiffusion, *Modern Phys. Lett. B* 23 (9) (2009) 1147–1155.
- [15] E.M. Lifschitz, L.P. Pitaevskii, *Physical Kinetics*, Butterworth-Heinemann, 1981.
- [16] C.A. Truesdell, *Rational Thermodynamics*, Springer-Verlag, New York, 1984.
- [17] B. Øksendal, *Stochastic Differential Equations*, 5th ed., in: Universitext, Springer-Verlag, Berlin, 1998.
- [18] R. Kippenhahn, A. Weigert, *Stellar Structure and Evolution*, 1st ed., in: Astronomy and Astrophysics Library, Springer-Verlag, Berlin, Heidelberg, New York, 1990.
- [19] W. van Leeuwen, S.R. de Groot, *Physica* 51 (1971) 16–31.
- [20] W. van Leeuwen, C.G. van Weert, S.R. de Groot, *Phys. Lett.* 47A (1974) 221–223.
- [21] A.J. Kox, W. van Leeuwen, S.R. de Groot, *Physica A* 84 (1976) 165–174.